

# STUDY ON THE INFLUENCE OF THE GROUND MOTION ON THE $R_a - R_d$ CURVE USING FIELD MEASUREMENT DATA

Ligang LI<sup>\*1</sup>, Masaomi TESHIGAWARA<sup>\*2</sup>, Akihiro NAKAMURA<sup>\*3</sup> and Toshihide KASHIMA<sup>\*4</sup>

## ABSTRACT

The  $R_a - R_d$  curve shows the relationship between rotation angle of the foundation (corresponding to  $R_d$ ) and the moment of the superstructure (corresponding to  $R_a$ ) during the earthquake, which can reflect the soil performance under the foundation. In this paper, we want to study the influence of the ground motion on the  $R_a - R_d$  curve using field measurement data for 7 strong earthquakes. The results show that the rotation motions of the ground surrounding the building are strong correlated with the accuracy of the  $R_a - R_d$  curve.

Keywords: SRC building, Performance curve, Ground motion, Wavelet Transform Technology

## 1. INTRODUCTION

Destructive earthquakes caused much serious earthquake damage of buildings, and that is the main reason of the large casualties. In order to recover the social order and make the refugees go back to their homes as soon as possible, the safety of the buildings should be confirmed. Therefore, a quick and effective evaluation method for the earthquake damage in main shocks and for the prediction of the residual seismic capacity (related with the collapse of the building) of the buildings in the aftershocks should be developed.

Currently, a method based on the performance curve, relationship between representative acceleration  $S_a$  and representative displacement  $S_d$ , has already been brought out to satisfy the requirement mentioned above [1]. Wavelet Transform Technique (WTT) is used to extract the fundamental response [2, 3], which can be used to obtain  $S_a - S_d$  curve. However,  $S_a - S_d$  curve is mainly for the seismic evaluation of the superstructure. Actually, the seismic performance of the soil should be evaluated in order to judge the risk of the overturn of the foundation. So we want to apply the concept of the  $S_a - S_d$  curve to get the relationship between rotational acceleration  $R_a$  and rotational angle of foundation  $R_d$  ( $R_a - R_d$  curve), which can reflect the seismic performance of soil during earthquakes.

Generally, the rotational angle of the foundation ( $R_d$ ) was calculated using the measurement response data of the base floor. That assumes that there is no influence of the rotational motion of the ground on  $R_d$ . However, there are many fluctuations in the  $R_a - R_d$  curve for the real buildings during strong earthquakes, see Figure 1. We infer that maybe the influence of the ground motion on  $R_a - R_d$  curve is important.

In this paper, massive measurement data of an

8-story Steel-Reinforced concrete (SRC) building for 7 strong earthquakes was studied. The research objective of the paper is to evaluate the influence of the rotational motion of the ground on the accuracy of the  $R_a - R_d$  curve.

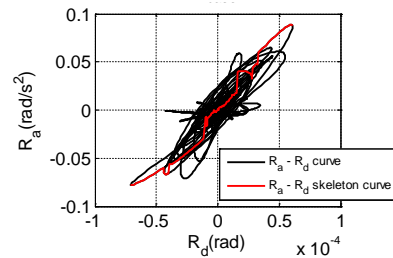


Fig. 1  $R_a - R_d$  curve of the building in N-S direction for the earthquake E7 shown in Table 1

## 2. FIELD MEASUREMENT DATAS

Just as shown in Figure 2, 11 accelerometers are installed in the building and another 5 accelerometers (A01, B01, C01, N14 and A14) are located in the shallow layers of the soil surrounding the building. Each accelerometer can record 3-direction motions (x direction: E-W, y direction: N-S and z direction: vertical direction). The sampling frequency of the accelerometers is 100Hz.

7 strong earthquakes that occurred in Japan between 1998 and 2012 were selected in this paper, see Table 1.

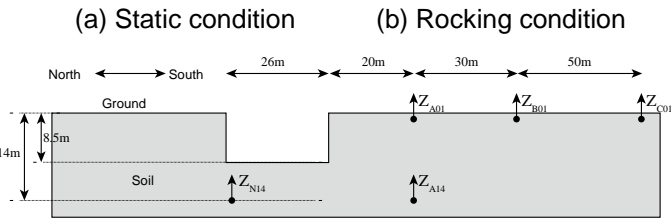
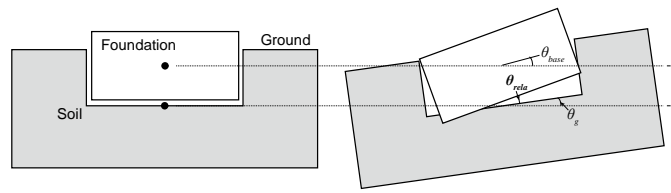
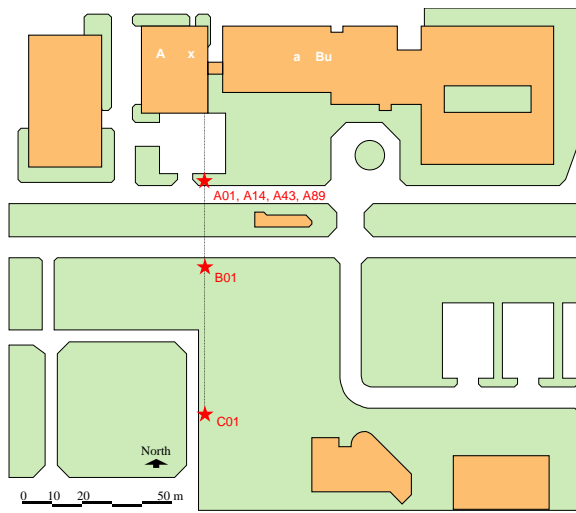
## 3. $R_a - R_d$ CURVE

According to methods given in the past research, the  $S_a - S_d$  curves of the building can be obtained. If we assumed that the rocking motion mainly couples with

\*1 Ph.D. Candidate of Graduate School of Environmental Studies, Nagoya University, JCI Student Member  
 \*2 Prof., Nagoya University, Dr. Eng. (Visiting Research Engineer, Building Research Institute), JCI Member  
 \*3 Assist Prof., Nagoya University, Dr. Eng., JCI Member  
 \*4 Senior Research Engineer, Building Research Institute

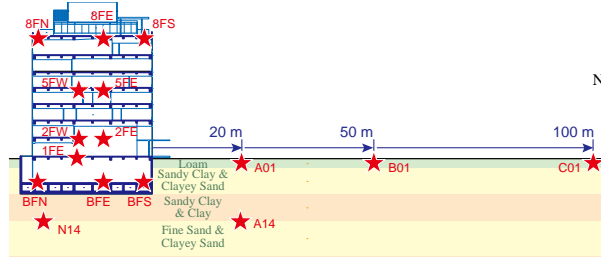
Table 1 7 Strong earthquakes that occurred in Japan between 1998 and 2012

| Time             | Epicenter                  | Latitude | Longitude | Depth (km) | M (Degree) | Dist. (km) | PGA (gal) | IJMA (Degree) | Fundamental response (N-S)   | Number |
|------------------|----------------------------|----------|-----------|------------|------------|------------|-----------|---------------|------------------------------|--------|
| 2003/09/20 12:54 | S Chiba Pref.              | 140.3033 | 35.2150   | 70         | 5.8        | 104        | 13.7      | 2.8           | rank6<br>[0.83-1.67Hz]       | E1     |
| 2004/10/06 23:40 | S Ibaraki Pref.            | 140.0917 | 35.9850   | 66         | 5.7        | 17         | 54.5      | 3.8           | rank6<br>[0.83-1.67Hz]       | E2     |
| 2005/08/16 11:46 | Off Miyagi Pref.           | 142.2783 | 38.1500   | 42         | 7.2        | 298        | 29.8      | 3.3           | rank6<br>[0.83-1.67Hz]       | E3     |
| 2008/06/14 08:43 | S Inland Iwate Pref.       | 140.8800 | 39.0283   | 8          | 7.2        | 330        | 26.2      | 3.4           | rank6<br>[0.83-1.67Hz]       | E4     |
| 2011/03/11 14:46 | Off Sanriku                | 142.8600 | 38.1033   | 24         | 9.0        | 330        | 279.3     | 5.3           | rank6+rank7<br>[0.42-1.67Hz] | E5     |
| 2011/03/11 15:15 | Off Ibaraki Pref.          | 141.2650 | 36.1083   | 43         | 7.6        | 107        | 151.1     | 4.7           | rank6<br>[0.83-1.67Hz]       | E6     |
| 2011/04/11 17:16 | Hama-dori, Fukushima Pref. | 140.6717 | 36.9450   | 6          | 7.0        | 105        | 118.1     | 4.6           | rank6<br>[0.83-1.67Hz]       | E7     |

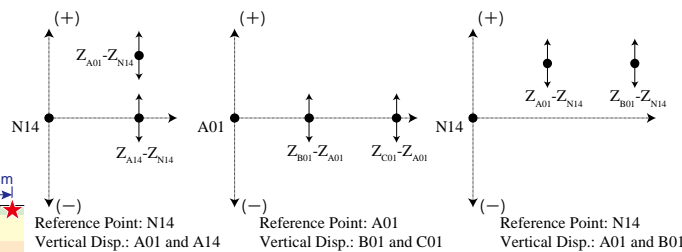


(c) Vertical motions of the measurement points  
Fig. 3 Concept of the rocking motion for the surrounding ground of the building in Figure 2

(a) Location of the building and accelerometers on the ground



(b) Locations of the accelerometers in the soil  
Fig. 2 Distribution of the accelerometers in the ground and the soil for the BRI Annex building



(a) Case 1 (b) Case 2 (c) Case 3  
Fig. 4 Concept of the Relative vertical displacements among the 5 measurement points

the fundamental mode. Then the representative rocking-moment coefficient  $R_a$  can be calculated as follows:

$$R_a = \frac{S_a}{H_e} \quad (1)$$

Where the equivalent height  $H_e$  is about 18.80m (the total height of the superstructure is 28m).  $R_d$  is the fundamental component of rotation angle of the foundation (WTT is applied to get fundamental component).

Then the relationship between  $R_a$  and  $R_d$  can be expressed as follows:

$$\omega_r = \sqrt{-\frac{R_a}{R_d}} \quad (2)$$

Where  $\omega_r$  is the fundamental circular frequency

for the rocking motion of the foundation.

#### 4. INFLUENCE OF THE GROUND MOTION ON THE $R_a - R_d$ CURVE

##### 4.1 Analysis on the vertical motion of the ground

In order to analyze the vertical motions of the ground, 5 measurement points (N14, 14 meters under the building; A01, B01 and C01, 1 meter under the ground; A14, 14 meters under the ground, see Figure 2) located in the soil were studied. The vertical motions of the 5 points were recorded during the earthquakes, and see Figure 3(c). The earthquake E7 was taken as the analysis sample in this section.

Just as what is shown in Figure 4, the 5 points are separated into three cases: (1) case 1, the reference point is N14, and the relative vertical motions of A01 and A14 are shown in Figure 5(a); (2) case 2, the reference point is A01, and the relative vertical displacements of B01 and C01 are shown in Figure 5(b); (3) case 3, the reference point is N14, and the relative vertical motions of A01 and B01 are shown in Figure 5(c). The vertical displacement of each point is calculated by the trapezoidal integration, and the base line modification.

According to the Figure 5, we found that almost at any time: (1) rotation motion exists between points N14 and A01, A14, and the rotation directions are almost same for A01 and A14; (2) rotation motion happens between points A01 and B01, C01, and rotation directions are almost same for B01 and C01; (3) rotation motion exists between points N14 and A01, B01, and rotation directions are almost same for A01 and B01. So it can be concluded that rotation motions of the ground existed surrounding the building, and the rotation motion (rocking angle) of the basement maybe contain the rotation motions (rotation angle) of the ground.

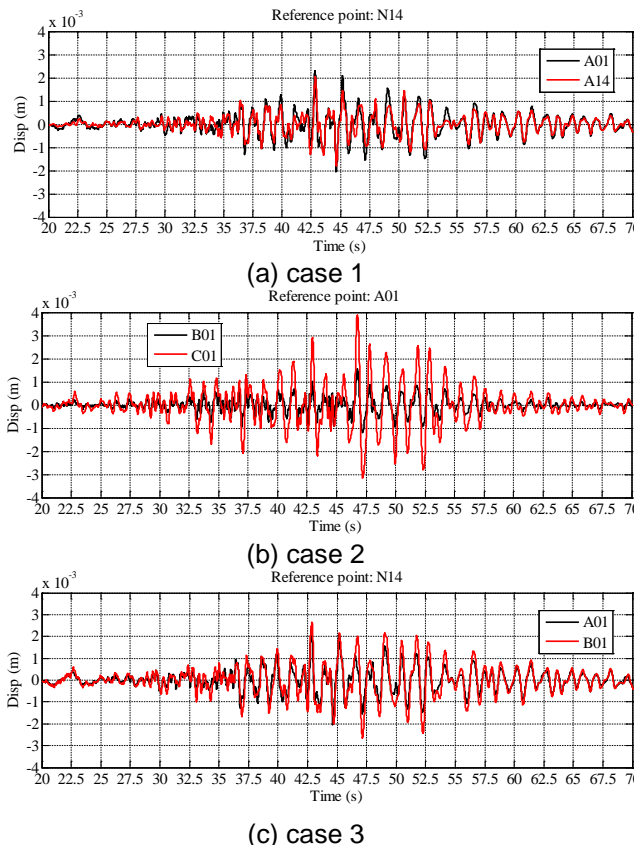


Fig. 5 Relative vertical displacements of the 3 cases of Figure 4 for earthquake E7 in NS direction

#### 4.2 Calculation of the rotation angle of the ground

As for the calculation of the rocking angle  $\theta_{base}$  of the building, we used the motions of the three points BFN, BFE and BFS located on the base floor, see Figure 2 (b). However,  $\theta_{base}$  reflects the absolute rocking motion of the foundation, which contains the

rotation motion of the ground. In order to get the  $R_a - R_d$  curve of the soil (reflects the relationship between the deformation of soil and the moment of the building), we should calculate the relative rotation angle  $\theta_{rela}$  between the foundation and its surrounding ground, see

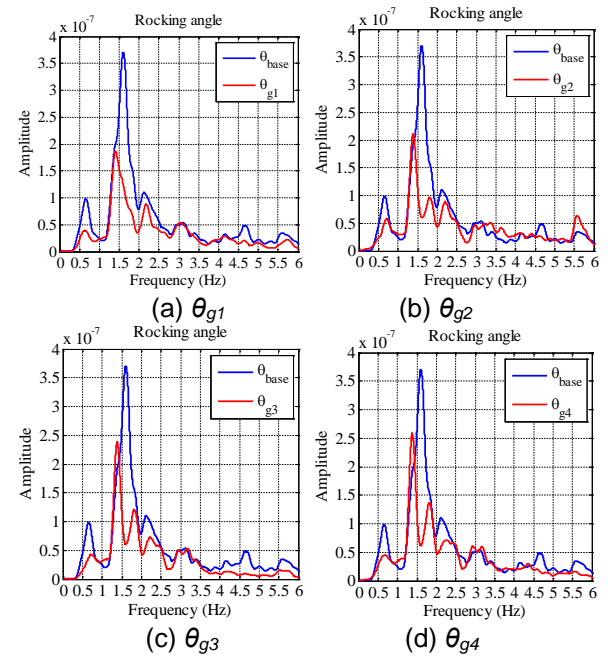


Fig. 6 Fourier spectrum of the  $\theta_g$  for earthquake E7 in N-S direction

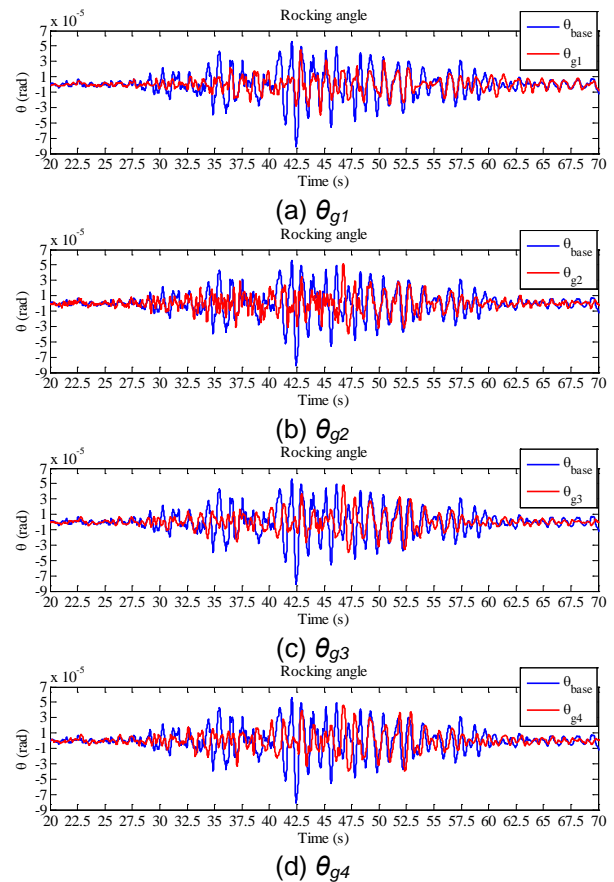


Fig. 7 Time history of the N-S direction rotation angles for earthquake E7

Figure 3 (b). There is a simple relationship between  $\theta_{base}$  and  $\theta_{rela}$  as follows,

$$\theta_{rela} = \theta_{base} - \theta_g \quad (3)$$

Where  $\theta_g$  is the rotation angle of the ground surrounding the foundation, see Figure 3(b). The vertical motions of the measurement points can be used to calculate  $\theta_g$ . For the case shown in Figure 2 and 3, five points (A14, N14, A01, B01 and C01) and four equations will be employed to calculate  $\theta_g$ , which are as follows, see Figure 4.

For points N14 and A14:

$$\theta_{g1} = \frac{Z_{A14} - Z_{N14}}{46} \quad (4)$$

For points A01 and B01:

$$\theta_{g2} = \frac{Z_{B01} - Z_{A01}}{30} \quad (5)$$

For points A01 and C01:

$$\theta_{g3} = \frac{Z_{C01} - Z_{A01}}{80} \quad (6)$$

For points B01 and C01:

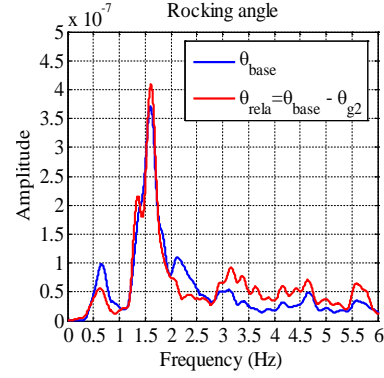
$$\theta_{g4} = \frac{Z_{C01} - Z_{B01}}{50} \quad (7)$$

Just as what is shown in Figure 6 and Figure 7, the rotation motions of the ground were strong compared with the rocking motion of the foundation in earthquake E7. Fourier spectrums (Figure 6) show that rotation motions  $\theta_{g2}$ ,  $\theta_{g3}$  and  $\theta_{g4}$  own the almost same frequency spectrums; but  $\theta_{g1}$  is a little different from the three rotation motions. The reason is maybe because of the locations of the measurement points. For example, the measurement points A01, B01 and C01 (used for the calculation of  $\theta_{g2}$ ,  $\theta_{g3}$  and  $\theta_{g4}$ ) are located in the free field ground; but A14 and N14 (for  $\theta_{g1}$ ) were under the ground, and the building was just above the point N14, see Figure 2(b).

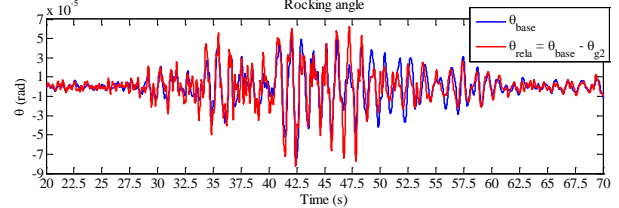
#### 4.3 Decision of the rotation motions of the ground surrounding the building

Based on previous analysis, we have already known that the rotation motions of the ground occurred during the earthquakes. As for the different rotation motions ( $\theta_{g1}$ ,  $\theta_{g2}$ ,  $\theta_{g3}$  and  $\theta_{g4}$ ), we do not know which one is the real input rotation motion. In this part, the influence of the different rotation motions of the ground on the shape of  $R_a - R_d$  curve of the foundation of the building was studied. The calculation model of the relative rocking angle  $\theta_{rela}$  can be found in Equation (3) and Figure 3 (a) and (b). The earthquake E7 was taken as the example. The comparison between the  $\theta_{base}$  (absolute rocking angle of the foundation) and the  $\theta_{rela}$  (relative rotation motion between the foundation and the surrounding ground,  $\theta_{g2}$  as the rotation motion of the ground) is shown in Figure 8.

The representative rocking angle  $R_d$  will be corresponding to  $\theta_{base}$  and  $\theta_{rela}$  respectively. Then Wavelet Transform Technology will be employed to get fundamental response of the rocking angle. Just as shown in Figure 9, five different cases for  $R_d$  (rank 6 as the fundamental response) were compared. Skelton curve, connected line of any point that update the maximum rotational angle due to the time history, is also shown in Figure 9. It can be found that the hysteresis loops of the  $R_a - R_d$  curve for  $\theta_{base} - \theta_{g2}$  (see Figure 9 (c)) are more compact than other cases. It is

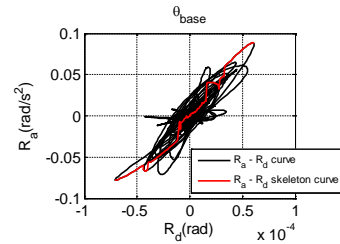


(a) Fourier spectrum of  $\theta_{rela}$  for E7 in NS direction

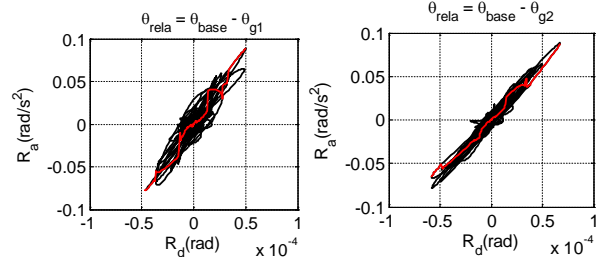


(b) Time history of  $\theta_{rela}$

Fig. 8 Relative rocking angle  $\theta_{rela}$  of the foundation to the ground for  $\theta_{g2}$  for E7 in NS direction

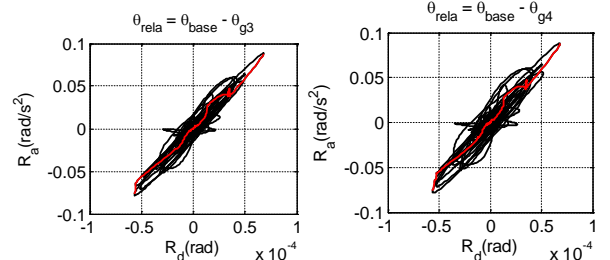


(a)  $R_d$  for  $\theta_{base}$



(b)  $R_d$  for  $\theta_{base} - \theta_{g1}$

(c)  $R_d$  for  $\theta_{base} - \theta_{g2}$



(d)  $R_d$  for  $\theta_{base} - \theta_{g3}$

(e)  $R_d$  for  $\theta_{base} - \theta_{g4}$

Fig. 9 Comparison of the influences of the different  $\theta_g$  of the ground on  $R_a - R_d$  for earthquake E7 in N-S direction

easy to conclude that the soil response is linear according to the Figure 9 (c), but it is difficult to get the same conclusion for other cases. The reason may be because of the locations of the measurement points.

We deemed that the rotation motions of the ground will be bad for the shape the  $R_a - R_d$  curve,

when the rotation motions of the ground are strong. In a sense, the rotation motions of the ground are kinds of noise. However, the  $R_a - R_d$  curve will be easy to be understood once the the rotation motions of the ground is deleted. In the next analysis,  $\theta_{g2}$  will be as the real input rotation motion of ground surrounding the building.

#### 4.4 Influence of $\theta_{g2}$ on the shape of the $R_a - R_d$ curve

As for the influence of the  $\theta_{g2}$  on the shape of the  $R_a - R_d$  curves, all the 7 earthquakes were discussed. Just as what is shown in Figure 10, when the rotation motion of the ground  $\theta_{g2}$  was deleted from the rocking motion of the foundation  $\theta_{base}$ , the hysteresis loops of the corresponding  $R_a - R_d$  curves would become compact and easy to understand. It can be easily concluded that the soil responses were linear during the earthquakes E1-E6. Besides, stronger rotation motion of the ground ( $\theta_{g2}$ ) always have larger influence on  $R_a - R_d$  curves.

A for earthquake E1, see Figure 11(a): Because  $\theta_{g2}$  was very small (Figure 10(a)) during the earthquake, so the influence of  $\theta_{g2}$  on the shape of  $R_a - R_d$  curve was very little.

For earthquake E2, E4, E5 and E6, see Figure 11(b), (d) and Figure 12 (a) and (b): the influence of  $\theta_{g2}$  on  $R_a - R_d$  curves was strong (Figure 10 (b), (d), (e) and (f)), but the influence of  $\theta_{g2}$  could almost be directly deleted.

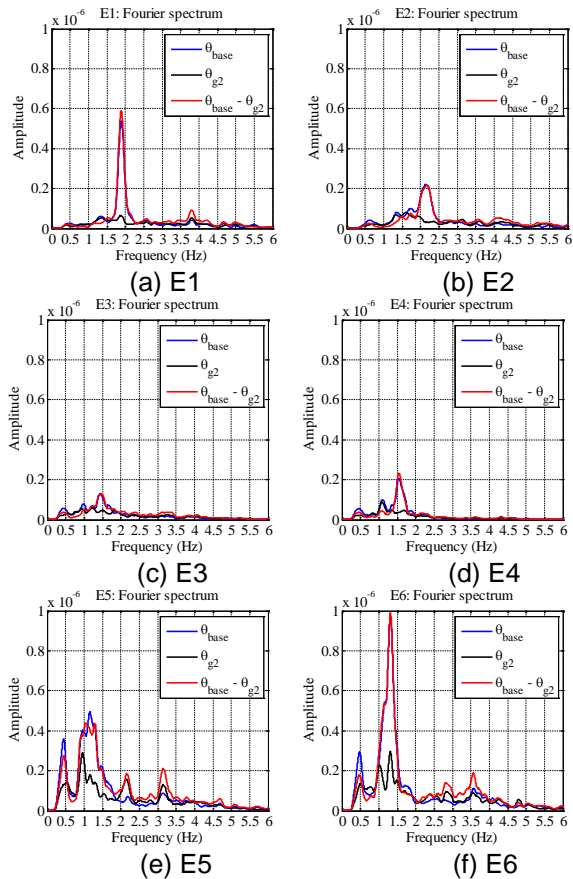


Fig. 10 Fourier spectrums of the rotation angles  $\theta_{base}$  and  $\theta_{g2}$  for each earthquake

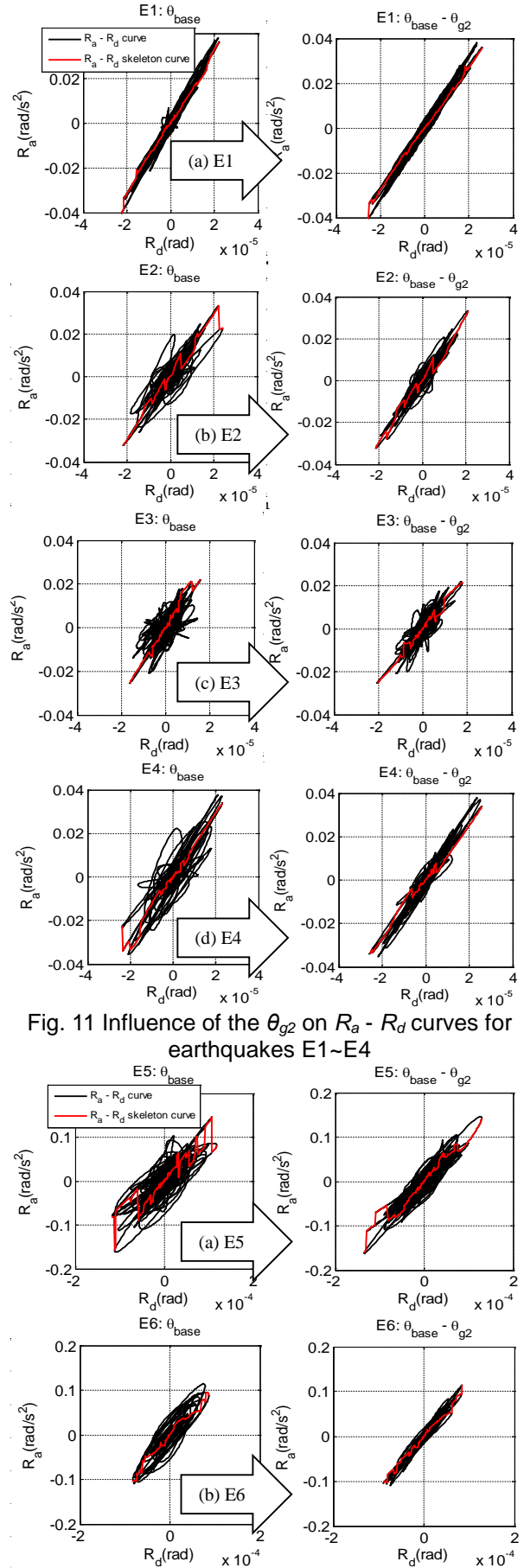


Fig. 11 Influence of the  $\theta_{g2}$  on  $R_a - R_d$  curves for earthquakes E1~E4

Fig. 12 Influence of the  $\theta_{g2}$  on  $R_a - R_d$  curves for earthquakes E5~E6

For earthquake E3, see Figure 11(c): it seems that influence of the rotation motion of the ground on the  $R_a - R_d$  curve is much more complex (Figure 11(c)); and the  $R_a - R_d$  curve did not become very compact after deleting  $\theta_{g2}$ . However, because the rocking motion is not strong compared with other earthquakes and the  $R_a - R_d$  skeleton curve shows the linearity of the soil response, it can be accepted that the soil response during the earthquake was linear.

#### 4.5 Influence of $\theta_{g2}$ on the fundamental frequency for the rocking motion

After deleting (means  $\theta_{base}-\theta_{g2}$ ) the influence of  $\theta_{g2}$ , the  $R_a - R_d$  curves and  $R_a - R_d$  skeleton curves become easier to understand and analyze. Because the soil responses for the 7 earthquakes were linear, so the maximum peak response points of the  $R_a - R_d$  curves were selected to calculate the fundamental frequency ( $f_r = \omega_r/2\pi$ ), and  $\omega_r$  was calculated by Equation (2).

The influence of  $\theta_{g2}$  on the fundamental frequency for the rocking motion in N-S direction was evaluated in Figure 12:  $\theta_{base}$  means  $f_r$  contains the influence of  $\theta_{g2}$ , and  $\theta_{base}-\theta_{g2}$  means  $f_r$  deletes the influence of  $\theta_{g2}$ . Some discussions were made as follows according to Figure 12:

(1) The approximate value of  $f_r$  is about 6.5Hz – 5.0Hz. And there is a trend that  $f_r$  decreased gradually from about 6.5 Hz to about 5.5 Hz for earthquakes E1~E7, especially according to the values in the Negative direction.

(2) For earthquakes E3, E6 and E7, the influence of  $\theta_{g2}$  on  $f_r$  is a little large in Positive direction of the response. But compared with the influence of  $\theta_{g2}$  on the hysteresis loops of the  $R_a - R_d$  curves, the influence of  $\theta_{g2}$  on  $f_r$  was maybe not so outstanding.

Totally, no matter deleting or without deleting  $\theta_{g2}$ , the maximum peak response points of the  $R_a - R_d$  curves can be used to calculate  $f_r$  (fundamental frequency of the foundation for rocking motion).

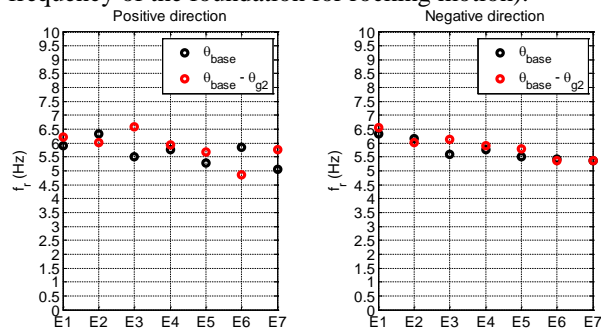


Fig. 13 Influence of  $\theta_{g2}$  on the fundamental frequency of the rocking motion of the foundation in N-S direction

## 5 DISCUSSION AND CONCLUSIONS

In this section, we analyzed the influence of the rotation motion on the  $R_a - R_d$  curve of the foundation in N-S direction. We found that although the rotation motion of the ground surrounding the building affected the hysteresis loops of the  $R_a - R_d$  curve very much (especially when the rotation motions of the ground surrounding the building were large), the influence of the rotation motion of the ground on  $f_r$  was not so large. Besides, rotation motion of the ground surrounding the building was decided by the locations of the measurement points.

In this research, we did not locate the measurement points in E-W direction, so no analysis was made on the influence of the rotation motion of the ground on the  $R_a - R_d$  curve in E-W direction.

## ACKNOWLEDGEMENT

This research was made possible by the Building Research Institute (BRI) of Japan, which supplied important original measurement data. The WTT program used in this research was supplied by Professor Koichi KUSUNOKI of the University of Tokyo

## REFERENCES

- [1] Koichi KUSUNOKI, Masaomi TESHIGAWARA and Eiji KOIDE: Development of real-time residual seismic capacity evaluation system No 1: Outline of the evaluation method, Summaries of Technical Papers of Annual Meeting Architectural Institute of Japan, Tokai, Japan, pp.961-962, 2003.
- [2] Manabu Kawamura, Koichi Kusunoki, Miho Yamashita, Yuki Kattori, Daiki Hinata, Miguel Augusto DIAZ FIGUEROA and Akira Tasai: Study of a New Method to Compute the Performance Curve of Real Structures with Acceleration Sensors in the case of SDOF System Structures, J. Struct. Constr. Eng. AIJ, No.688, pp.1061–1069, 2013.6.
- [3] Koichi Kusunoki, Daiki Hinata, Yuki Hattori, and Akira Tasai: Development of a new method of realtime residual seismic capacity evaluation of existing structures with accelerometers in the case of MDOF system structures, J. Struct. Constr. Eng., AIJ, No. 699, pp. 613–620, 2014.5.